In vivo analysis of human nucleoporin repeat domain interactions

Songli Xu* and Maureen A. Powers
Department of Cell Biology, Emory University School of Medicine, Atlanta, GA 30322

ABSTRACT The nuclear pore complex (NPC), assembled from ~30 proteins termed nucleoporins (Nups), mediates selective nucleocytoplasmic trafficking. A subset of nucleoporins bear a domain with multiple phenylalanine–glycine (FG) motifs. As binding sites for transport receptors, FG Nups are critical in translocation through the NPC. Certain FG Nups are believed to associate via low-affinity, cohesive interactions to form the permeability barrier of the pore, although the form and composition of this functional barrier are debated. We used green fluorescent protein–Nup98/HoxA9 constructs with various numbers of repeats and also substituted FG domains from other nucleoporins for the Nup98 domain to directly compare cohesive interactions in live cells by fluorescence recovery after photobleaching (FRAP). We find that cohesion is a function of both number and type of FG repeats. Glycine–leucine–FG (GLFG) repeat domains are the most cohesive. FG domains from several human nucleoporins showed no interactions in this assay; however, Nup214, with numerous VFG motifs, displayed measurable cohesion by FRAP. The cohesive nature of a human nucleoporin did not necessarily correlate with that of its yeast orthologue. The Nup98 GLFG domain also functions in pore targeting through binding to Nup93, positioning the GLFG domain in the center of the NPC and supporting a role for this nucleoporin in the permeability barrier.

INTRODUCTION

In eukaryotic cells, trafficking between the nucleus and cytoplasm occurs through the nuclear pore complex (NPC), a massive structure that spans the nuclear envelope. The NPC is built of repeating subcomplexes made from ~30 proteins termed nucleoporins (Nups; Hoelz et al., 2011; Onischenko and Weis, 2011). NPCs are selective channels, facilitating the passage of large cargoes that display specific targeting signals (e.g., nuclear localization sequence [NLS]; nuclear export sequence [NES]). These signals are recognized by a large family of mobile receptors termed karyopherins, also referred to as importins, exportins, or transportins (reviewed in Hutten and Kehlenbach, 2007; Chook and Suel, 2011; Marfori et al., 2011). Molecules less than ~40 kDa in size freely diffuse through the pore with no requirement for signals or receptors.

The ability of the NPC to selectively translocate large cargoes yet permit free passage of smaller proteins is remarkable, and a subset of nucleoporins are integral to these processes (Terry and Wente, 2009; Walde and Kehlenbach, 2010). Such phenylalanine–glycine (FG) repeat nucleoporins are each characterized by a domain containing multiple copies of the FG motif or its variants, in vertebrates primarily FxFG (where x is any amino acid), glycine–leucine–FG (GLFG), or proline–xFG (PxFG). Spacer sequences separate individual motifs; these spacers lack a consensus sequence but are generally enriched in serine, threonine, and proline (S, T, and P, respectively). Of importance, nucleoporin repeat domains are intrinsically disordered (Bayliss et al., 2000; Denning et al., 2003; Patel et al., 2007). FG nucleoporins are present throughout the NPC, on cytoplasmic filaments, on the nuclear basket, and, especially, lining the central channel. Because nucleoporins are typically present in 8 or 16 copies due to the eightfold symmetry of the NPC, it is estimated that there are >100 repeat domains and thus thousands of FG motifs in each pore (Rout et al., 2000; Strawn et al., 2004).

Abbreviations used: BSA, bovine serum albumin; DTT, dithiothreitol; FG, phenylalanine–glycine; FRAP, fluorescence recovery after photobleaching; FxFG, phenylalanine–any amino acid–phenylalanine–glycine; GBD, Gle2-binding domain; GLEBS, Gle2-binding sequence; GLFG, glycine–leucine–phenylalanine–glycine; HD, 1,6 hexanediol; NES, nuclear export signal; NLS, nuclear localization sequence; NPC, nuclear pore complex; PBS, phosphate-buffered saline; PxFG, proline-any amino acid-phenylalanine-glycine.

Efficient translocation of karyopherin receptor–cargo complexes through the NPC occurs via interactions between the receptor and the FG repeat domains. FG repeat nucleoporins are also believed to be responsible for the permeability barrier of the NPC, although this function is less well understood (Ribbeck and Gorlich, 2002). The permeability barrier must permit diffusion of molecules less than ~40 kDa, exclude large noncargo molecules, and simultaneously be penetrable by transport receptors during translocation of cargo. Multiple models for NPC organization have been proposed to account for these somewhat paradoxical requirements (Ribbeck and Gorlich, 2001; Rout *et al.*, 2003; Peters, 2005; Frey *et al.*, 2006; Lim *et al.*, 2007). Although models differ in some major aspects, both the selective phase (Frey *et al.*, 2006) and forest (Yamada *et al.*, 2010) models have as a key feature the relative tendencies of different FG-repeat domains to participate in low-affinity, intramolecular and intermolecular cohesive interactions (reviewed in Walde and Kehlenbach, 2010; Yang, 2011).

Cohesive interactions of repeat domains are mediated by their FG motifs but are also influenced by the composition of the spacer regions that lie between these motifs (Patel *et al.*, 2007; Yamada *et al.*, 2010). Repeat domain interactions are of low affinity, in keeping with the necessarily dynamic nature of the permeability barrier of the NPC. However, this low affinity has made in vitro analysis of these interactions problematic. Cohesive interaction between repeat domains has been studied most systematically using FG domain fragments from yeast nucleoporins. A sensitive binding assay (Patel *et al.*, 2007), combined with measurement of hydrodynamic properties of FG domains, led to the forest model, in which cohesive FG domains adopt a globular, collapsed-coil conformation, whereas noncohesive repeat domains exhibit a more dynamic, extended-coil organization (Yamada *et al.*, 2010). Highly concentrated preparations of yeast FG domain fragments could be induced to form hydrogels in vitro that mimic some permeability properties of the NPC, in support of the selective phase model (Frey *et al.*, 2006). A fragment of the human Nup153 repeat domain was observed to collapse from an extended polymer to a more compact structure upon binding to importin β (Lim *et al.*, 2007). However, generally, the repeat domains of higher eukaryotes have proven much less amenable to recombinant expression and in vitro analysis.

Here we overcome these difficulties by exploiting leukemogenic Nup98/HoxA9 fusion proteins to investigate the cohesive properties of mammalian FG repeat domains in vivo. We compare several FG repeat domains for their propensity to form nucleoplasmic bodies and their relative cohesiveness in live cells. We find GLFG domains to be substantially more cohesive than domains carrying other types of repeats and the strength of the interaction to be a function of the number of repeat motifs within a domain. Among FxFG domains, Nup214 displays lower but measurable cohesion, in contrast to Nup62 and Nup153, which are noncohesive in this context. We further demonstrate that the GLFG domain of Nup98 interacts with the nonrepeat nucleoporin, Nup93. Whereas cohesive interactions between repeats, like the permeability barrier of the NPC, are sensitive to treatment with hexanediol (Ribbeck and Gorlich, 2002; Shulga and Goldfarb, 2003), binding between Nup98 and Nup93 is insensitive, as is the GLFG-dependent targeting of Nup98 to the NPC.

RESULTS

The number of FG repeats determines interaction between Nup98 and leukemic Nup98 fusion proteins

Previously we reported that the leukemogenic Nup98/homeodomain fusion proteins recruit endogenous Nup98 from GLFG bodies to the many finely punctate foci typically formed by the fusion
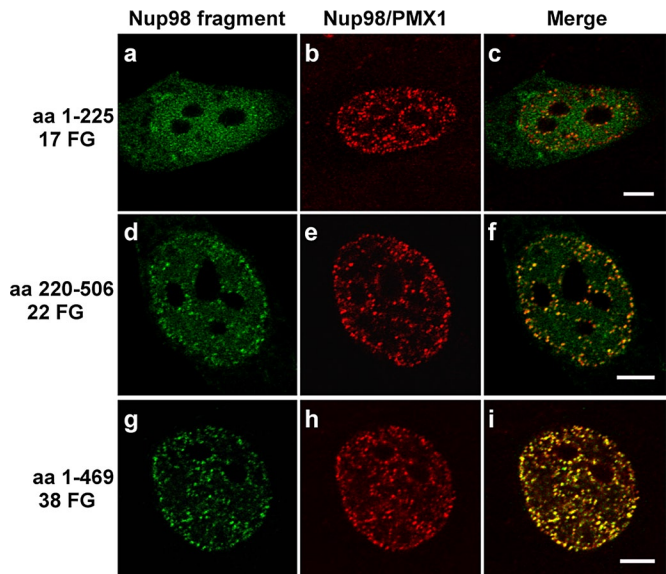
FIGURE 1: Association between Nup98 and leukemogenic Nup98 fusion proteins is a function of FG repeat number. GFP-Nup98 fragments (green) containing various numbers of nucleoporin FG repeat motifs (indicated as the total of all FG, FxFG, and GLFG motifs) were cotransfected with the CFP-tagged leukemogenic fusion protein Nup98/PMX1 (false colored in red) and visualized by confocal microscopy. The merged signal is shown at the right. Scale bars, 5 μm.

proteins (Xu and Powers, 2010). The functional significance of these intranuclear foci remains uncertain, although we hypothesize that the formation of foci through the association of repeats mimics interactions that would normally occur between repeat domains at the NPC. We tested various Nup98 fragments for in vivo interaction and found that the extent of association between Nup98 and Nup98/PMX1 correlated with the number of FG repeats encoded by the Nup98 construct (Figure 1). Nup98(1–225) corresponds to the N-terminal repeat region together with the binding site for Rae1/Gle2 (GBD or GLEBS; Pritchard *et al.*, 1999) and contains a total of 17 FG repeats. When expressed independently, this fragment did not form bodies (Griffis *et al.*, 2002) nor did it associate with the coexpressed Nup98/PMX1 (Figure 1, a–c). In contrast, the central repeat domain, which contains 22 FG repeats, formed GLFG bodies (Griffis *et al.*, 2002) and showed significant colocalization with Nup98/PMX1 (Figure 1, d–f). Association between a Nup98 fragment containing 38 FG repeats and Nup98/PMX1 was even more extensive (Figure 1, g–i).

Formation and dynamics of nuclear foci are a function of the number of FG repeat motifs

These results indicated that the extent of interaction between the Nup98 fragments and the Nup98/homeodomain fusion proteins was a function of the number of copies of the nucleoporin repeat motif, FG, or its variant, GLFG. It therefore seemed likely that all interactions between forms of Nup98, either formation of GLFG bodies by the endogenous protein or assembly of Nup98/homeodomain fusions into intranuclear foci, depend on association between repeat motifs. To test this possibility, we used a series of Nup98 constructs containing various numbers of repeats fused to another homeodomain, that of HoxA9 (Figure 2A). Nup98/homeodomain fusion proteins do not localize to the NPC since they lack the major targeting sequence of

the C-terminus (Xu and Powers, 2010). Therefore such fusions can be used to measure relative cohesiveness of repeat domains in vivo without influence of the NPC environment. The Nup98/HoxA9 constructs, fused to green fluorescent protein (GFP) for detection, were characterized by localization (Figure 2B) and fluorescence recovery after photobleaching (FRAP; Lippincott-Schwartz *et al.*, 2001; Dundr and Misteli, 2003) analysis of their dynamics (Figure 2C). Nup98, with its C-terminal NPC-targeting domain and 39 FG repeats, was found at the nuclear rim and in intranuclear bodies, whereas the C-terminus of HoxA9, which contains the homeodomain but no FG motifs, was found diffusely throughout the nucleus (Figure 2B). Between these extremes, as the number of FG repeats increased, the proteins displayed less diffuse and more organized distributions. Constructs with 9 (Figure 2B, c) or 17 FGs (not shown) were very similar in localization to the HoxA9 C-terminus. However, at 21 FGs, Nup98-GLFG/HoxA9 began to coalesce (Figure 2B, d). The 26 FG–containing construct clearly associated to form foci, although these were not as tightly focused as those formed by the leukemic Nup98/HoxA9 protein with 38 FG motifs (Figure 2B, e and f).

As an indication of relative affinities, we assessed the mobility of these fusion proteins by FRAP (Figure 2C). The recovery curves for proteins with 17–21 FG repeats were essentially indistinguishable, although as a group they were somewhat slowed compared with a protein with only 9 FG motifs. At 26 FGs, a significant reduction in recovery kinetics was observed, indicative of tighter interactions within the foci. Recovery curves were slower still when constructs contained 38 or 39 FG motifs. To further test the relationship between cohesiveness and FG repeats, we fused two copies of the central repeat domain of Nup98 to generate a construct with 43 FG motifs. This protein recovered even more slowly. Of importance, differences in recovery curves were not simply a function of protein molecular weight. The 21- and 26-FG constructs differ by only ~1.5 kDa, whereas the 38- and 39-FG fusions differ by ~17 kDa, and the 2× GLFG protein with 43 FG motifs is smaller than either. We conclude that binding affinity in foci is largely a function of the number of FG repeats, with a threshold for interaction occurring at 21–26 repeat motifs.

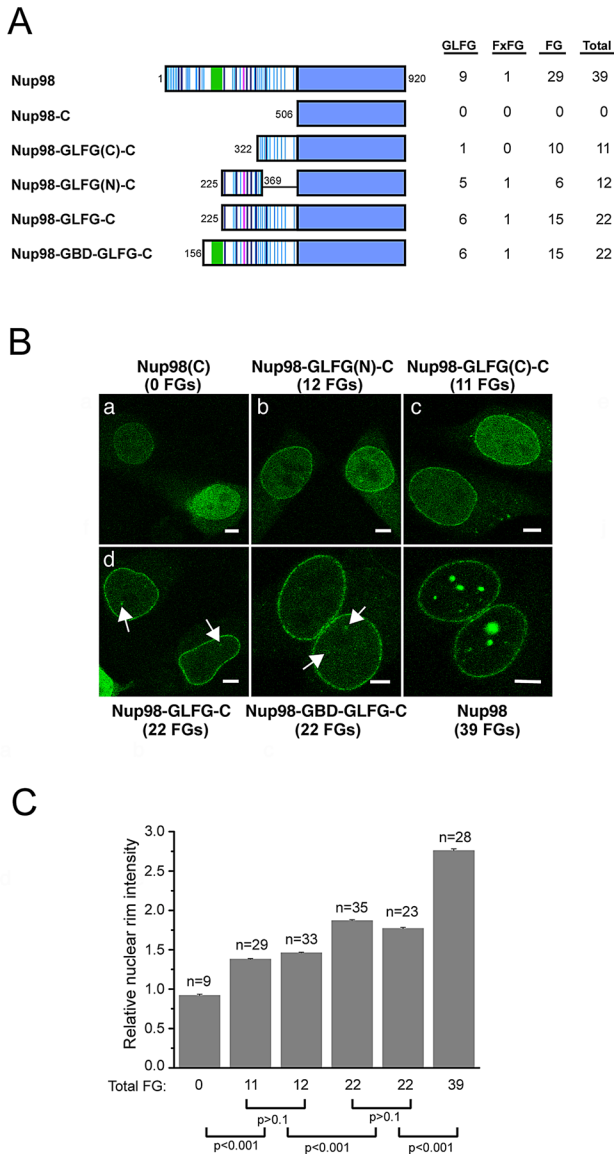## Stabilization of Nup98 at the NPC is correlated with number and type of repeats

Experiments to this point were focused on the interactions of FG motifs in the nucleoplasm. In earlier studies we showed that the central repeat domain of Nup98 contributes to NPC targeting in cooperation with the major targeting site in the C-terminal (Griffis *et al.*, 2003; Yoshida *et al.*, 2011). Using a series of Nup98 constructs with various numbers of FG repeats joined to the C-terminus (Figure 3A), we asked whether targeting of Nup98 to the NPC was also a function of repeat number. As illustrated (Figure 3B) and quantified (Figure 3C), targeting to the NPC showed a dependence on the number of repeats; however, the threshold of this effect appeared to be lower than that observed for intranuclear foci. Either half of the central repeat domain was sufficient to enhance NPC association; however, the full domain, with substantially more repeat motifs, had a greater effect. The ability of the Nup98 construct to interact with the dynamic nucleoporin Rae1/Gle2 had no influence on NPC association (Figure 2, B, compare d and e, and C).

Properties of repeat domains from other nucleoporins differ significantly from those of Nup98

We hypothesized that these assays for cohesion and enhancement of NPC targeting could be applied to other nucleoporin repeat
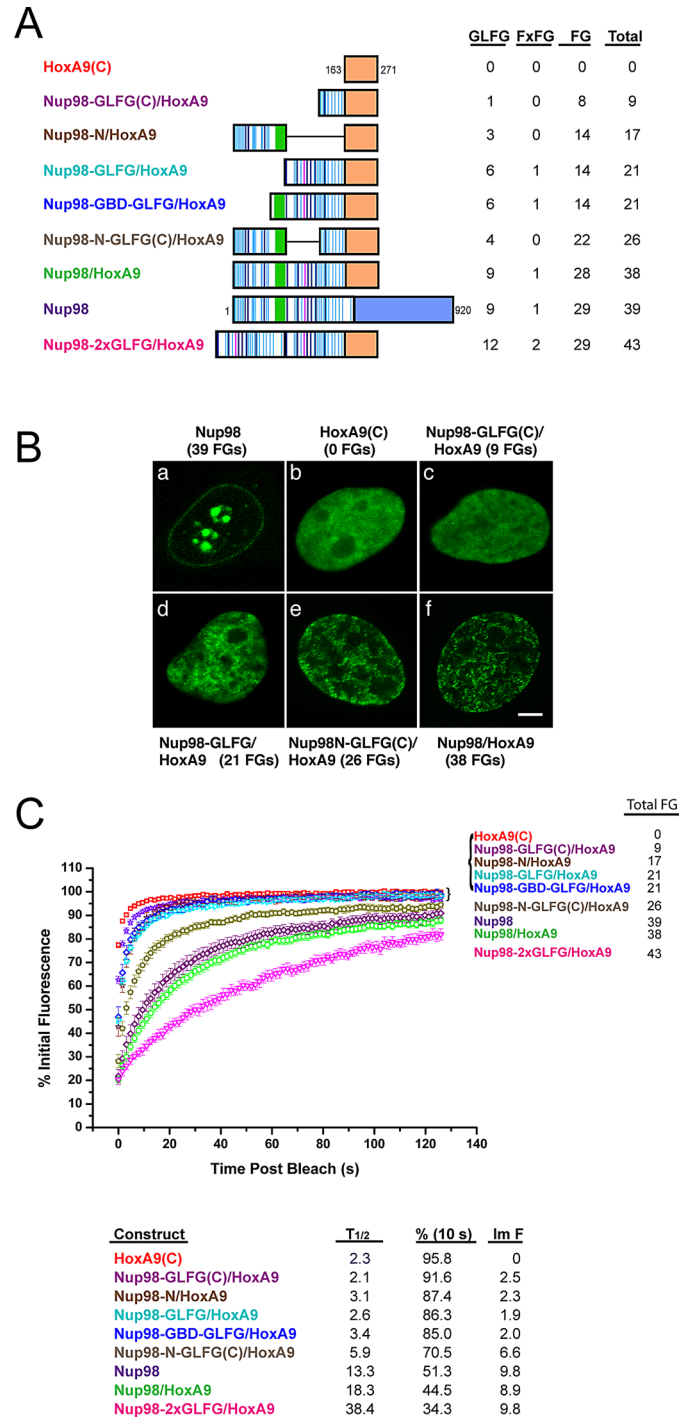
FIGURE 2: FG repeat number determines the affinity (cohesiveness?) of Nup98 fusion proteins. (A) Schematic of the different Nup98/HoxA9 constructs. FG repeats are indicated in light blue, GLFG repeats are in dark blue, and the single FXFG motif is in magenta. Repeats are positioned to scale, and the number of each type is indicated at right. (B) Localization of GFP-tagged exogenous Nup98, HoxA9 C-terminus, or Nup98/HoxA9 fusion proteins containing various numbers of repeats visualized by confocal microscopy. Number indicates total repeat motifs. Scale bar, 5 µm. (C) Dynamics of Nup98 fusion proteins with various numbers of FG motifs. GFP-tagged constructs were expressed in HeLa cells and photobleached, and fluorescence recovery was recorded over time. Curves are the average of at least six cells from two or more experiments. Error bars, SEM. Half-time of recovery, percent recovery at 10 s, and immobile fraction are indicated.

A

	GLFG	FxFG	FG	Total
Nup98 1 — 920	9	1	29	39
Nup98-C 506	0	0	0	0
Nup98-GLFG(C)-C 322	1	0	10	11
Nup98-GLFG(N)-C 225 — 369	5	1	6	12
Nup98-GLFG-C 225	6	1	15	22
Nup98-GBD-GLFG-C 156	6	1	15	22

B

Nup98(C) (0 FGs)   Nup98-GLFG(N)-C (12 FGs)   Nup98-GLFG(C)-C (11 FGs)

Nup98-GLFG-C (22 FGs)   Nup98-GBD-GLFG-C (22 FGs)   Nup98 (39 FGs)

C

Relative nuclear rim intensity

Total FG: 0 (n=9), 11 (n=29), 12 (n=33), 22 (n=35), 22 (n=23), 39 (n=28)

p>0.1 ; p>0.1 ; p<0.001 ; p<0.001 ; p<0.001

FIGURE 3: The contribution of the Nup98 repeat domain to NPC targeting is a function of the number of repeat motifs. (A) Schematic of the different Nup98 expression constructs. All constructs contain the full Nup98 C-terminal domain, which provides the major NPC-targeting motif. The number of each class of repeat motif is indicated at right. (B) Localization of GFP-tagged Nup98 constructs containing various numbers of repeats, as in A, visualized by confocal microscopy. Numbers indicate the total of all repeat motifs. Scale bar, 5 μm. (C) Quantification of NPC targeting. Low-expressing cells were chosen for analysis to minimize the formation of intranuclear bodies. Arrows indicate faint GLFG bodies seen at higher numbers of repeats. The relative nuclear rim intensity was scored as the ratio of nuclear rim intensity to intranuclear intensity in order to control for variation in cell-to-cell expression level. Between 9 and 35 individual cells were quantified for each construct as indicated. Statistically significant differences are indicated with p values. The relative nuclear rim intensity value for Nup98 with 39 repeats is somewhat inflated due to the strong propensity of nucleoplasmic protein to form GLFG bodies.

domains to compare their properties in vivo. To test this idea, we chose repeat domains from other nucleoporins (Figure 4A; see Supplemental Tables S1 and S2 for comparative properties of all human
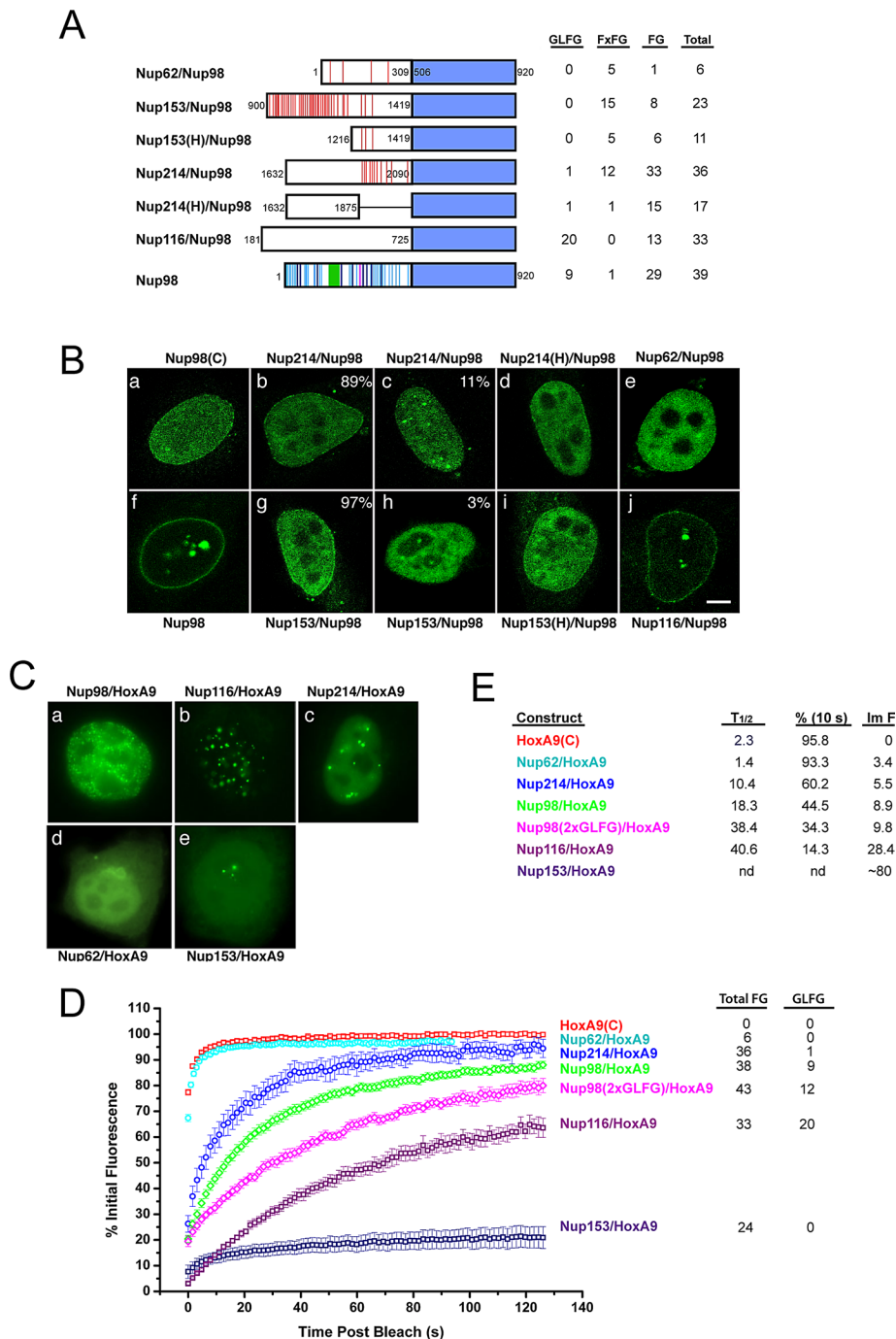
and yeast FG nucleoporin repeat domains) from different regions of the NPC and with differing levels of expected cohesiveness as estimated by Rexach and colleagues (Patel *et al.*, 2007). Nup62 is located within the central core of the NPC, and its repeat domain, with FxFG motifs and spacers rich in P, S/T, and G but low in charged residues, is predicted to be cohesive. Nup214 is found on the cytoplasmic filaments of the pore and contains mostly FG motifs, as well as variants including 10 PxFG motifs. Overall Nup214 was predicted to have a cohesive repeat domain (Patel *et al.*, 2007); however, there are several distinct regions within the Nup214 repeat domain, including one in which FG motifs are separated by charged spacers, followed by a cluster of PxFG repeats. Nup153 forms part of the nuclear basket of the NPC, and its repeat domain contains primarily FxFG motifs with one cluster of six PxFGs. Much of the Nup153 repeat domain has highly charged spacer sequences, and overall it is predicted to be noncohesive. Nup98, with GLFG and FG repeats, had a predicted intermediate degree of cohesiveness (Patel *et al.*, 2007). These initial predictions, based on binding data from yeast repeat domain fragments, have been further refined in a more recent, extensive study of the physical organization of yeast nucleoporin repeat domains (Yamada *et al.*, 2010).

The repeat domain of each nucleoporin was first fused to the C-terminal domain of Nup98 to determine whether other classes of repeats could enhance NPC targeting via the Nup98 C-terminus (Figure 4). Of interest, the Nup214, Nup62, and Nup153 repeat domains were unable to enhance NPC targeting (Figure 4B, b and c, e, and g and h, respectively). We did note that in a small percentage of cells, some Nup214/Nup98 C-term fusion protein was found in nucleoplasmic foci reminiscent of GLFG bodies (11%; Figure 4B, c). In contrast, the Nup153/Nup98 C-term fusion associated with foci in only 3% of cells, and these foci were always within the nucleolus. The Nup62/Nup98 C-term fusion protein was distributed throughout the nucleoplasm. Strikingly, when the repeat domain from Nup116, a yeast GLFG nucleoporin and one of the three Nup98 orthologues in *Saccharomyces cerevisiae*, was substituted for the repeat domain of Nup98 the pattern was identical to that of Nup98 (Figure 4B, f and j).

These results established that in vivo properties of the repeat domains of Nup214, Nup153, and Nup62 differ substantially from those of the GLFG repeat domains of Nup98 and Nup116. The ability to enhance NPC targeting is specific to GLFG nucleoporins, even though the Nup153 and Nup214 domains (with 23 and 36 FGs, respectively) possess well over the minimum number of FGs required for this function in Nup98 (Figure 2B). In addition, the repeat domains of Nup214 and Nup153 show very limited tendency to associate as intranuclear foci.

For Nup153 especially, but also in Nup214, spacer sequences in one region of the repeat domain are very rich in charged amino acids, especially lysine (Mackay *et al.*, 2010; Chow *et al.*, 2012). To investigate whether such a highly charged region might prevent association between repeats, we prepared constructs lacking the charged region of each repeat domain. This change did not enhance NPC targeting and only served to prevent the formation of any nucleoplasmic foci, perhaps due to the reduced number of repeats (compare Figure 4B, d and i with b and g).

To compare the relative cohesiveness of different domains, we returned to HoxA9 fusion proteins, since they are not targeted to the NPC where other nucleoporins might influence their behavior, and their distribution in the nucleoplasm facilitates assessment of binding by FRAP. The HoxA9 C-terminus alone is found diffusely throughout the nucleoplasm. In comparing the different repeat domains fused to the common HoxA9 C-terminus, differences in

FIGURE 4: Repeat domains from non-GLFG nucleoporins are not functionally equivalent to Nup98 repeats. (A) Schematic of constructs containing FG repeat domains from different nucleoporins as indicated fused to the Nup98 C-terminus (dark blue). Charged amino acids within the repeat domains are indicated by red bars. The number of each class of nucleoporin repeat motif is indicated at the right. (B) Localization of GFP-tagged constructs from A by confocal microscopy. Nup214/Nup98 and Nup153/Nup98 each resulted in two classes of localization pattern (b and c, and g and h, respectively), and the percentage of cells exhibiting each pattern is given at the upper right. Scale bar, 5 μm. (C) Nucleoporin repeat domains as in A were fused to the HoxA9 C-terminus in place of Nup98. GFP-tagged constructs were localized by widefield microscopy. Scale bar, 5 μm. (D) FRAP recovery curves for repeat domains fused to the HoxA9 C-terminus. Nup214/HoxA9 and Nup153/HoxA9 curves represent FRAP of intranuclear and intranucleolar bodies, respectively. Curves are the average of 6 to 19 cells from two or more experiments. Data sets used for HoxA9(C), Nup98/HoxA9, and Nup98(2xGLFG)/HoxA9 are the same as those used in Figure 2. Error bars, SEM. (E) Quantitation of FRAP curves, as in Figure 2C.

localization pattern and affinity, as observed by FRAP, were striking (Figure 4, C and D). As always, the leukemic Nup98/HoxA9 fusion protein associated in fine foci throughout the nucleus. Nup62/HoxA9 was found throughout the cell, with the highest concentration in the nucleoplasm. By FRAP analysis, Nup62/HoxA9 was a highly mobile protein with a recovery curve similar to that of the C-terminal domain of HoxA9. Thus, in this assay, Nup62 repeats show no tendency to associate. Nup153/HoxA9 was also distributed throughout the cell; indeed it was often difficult to discern the boundary of the nucleus, suggesting that it equilibrated freely between nucleus and cytoplasm. Like Nup62/HoxA9, the nucleoplasmic fraction of the Nup153/HoxA9 fusion was highly mobile (unpublished data). When Nup153/HoxA9 did form bodies, these were invariably within the nucleolus and showed little recovery after photobleaching (Figure 4D). Their behavior suggests that these may be nondynamic protein aggregates.

In contrast, a substantial number of cells expressing Nup214/HoxA9 contained bodies reminiscent of endogenous Nup98 GLFG bodies. Of interest, when compared with the far lower frequency of body formation by the Nup214/Nup98 C-term protein, this suggested that the behavior of these repeats is somewhat context sensitive. FRAP analysis revealed that Nup214/HoxA9 exchanged in and out of these assemblies with a recovery rate faster than Nup98/HoxA9 but significantly less than that of the freely mobile HoxA9 C-terminus (Figure 4, C, c, and D). Thus, in the context of a HoxA9 fusion, the Nup214 repeat domain behaved somewhat similarly to the Nup98 repeat domain but with significantly lower affinity, reflecting the difference in repeat composition. When the yeast Nup116 repeat domain was fused to HoxA9, recovery was markedly slower than even the 2× GLFG construct. With fewer total repeats but a much higher ratio of GLFG-to-FG motifs (61 vs. 28% for the 2× GLFG construct), the Nup116 domain was significantly more cohesive in its behavior. As in Figure 2, the relative rates of recovery were not proportional to the protein molecular weight.

The Nup98 GLFG repeat domain participates in two distinct interactions

Although these experiments clearly link the number of repeat motifs to the propensity for a nucleoporin to form intranuclear bodies, they do not formally distinguish between self-association of a GLFG nucleoporin through cohesive repeat motifs and binding

of a repeat nucleoporin to an unidentified protein partner. In the nuclear pore, repeat motifs are believed to produce a selective permeability barrier, although it is not resolved how many different nucleoporins contribute to this barrier. Function of the permeability barrier can be disrupted by treatment of cells with mild alcohols, such as 1,6-hexanediol (HD), which presumably dissociates the hydrophobic interactions between repeat motifs (Ribbeck and Gorlich, 2002; Shulga and Goldfarb, 2003; Patel *et al.*, 2007). To test whether HD disrupts Nup98 intranuclear foci, we observed the localization of proteins before and after treatment with HD (Figure 5A). Strikingly, in the presence of HD, the localization of Nup98 or Nup116 to intranuclear foci was completely abrogated. In contrast, constructs that localized to the NPC retained this association. The effect of HD treatment was confirmed using endogenous Nup98 in a cell line with a high frequency of GLFG bodies (HeLa-C; Xu and Powers, 2010). The endogenous Nup98 population at the NPC remained, but intranuclear Nup98 was dispersed throughout the nucleoplasm (Figure 5B).

The persistence of Nup98 at the NPC indicated that the GLFG repeat domain also participated in HD-resistant interactions. Further, the requirement for GLFG repeats to synergize with the Nup98 C-terminus suggested that this might involve a specific interaction rather than comingling of repeat domains into a heterogeneous hydrophobic gel or mesh. In *S. cerevisiae*, the nonrepeat nucleoporin Nic96 interacts with the GLFG domains of Nup57 and Nup49, members of a subcomplex, together with the FxFG nucleoporin, Nsp1 (Patel *et al.*, 2007; Schrader *et al.*, 2008). In metazoans, the orthologous complex consists of Nup62, Nup58, and Nup54, all of which contain FxFG or FG rather than GLFG repeats (Guan *et al.*, 1995; Hu *et al.*, 1996). The significance of this difference is uncertain, but as a result Nup98 is the only metazoan nucleoporin with significant GLFG motifs. To determine whether interaction with Nup93, the metazoan orthologue of Nic96, accounts for the HD-resistant interaction, we first tested whether Nup98 and Nup93 could be coimmunoprecipitated. Antibody to either protein was able to isolate the other (Figure 6A). To confirm that this interaction was a function of the repeat domain, we translated myc-tagged Nup98 or Nup98 fragments and tested them for binding to Nup93. Only variants that contained GLFG and FG repeat motifs were able to interact with Nup93 (Figure 6B). Finally, to determine whether interaction with Nup93 is resistant to HD, we coimmunoprecipitated Nup98 and Nup93 and washed them with buffer containing HD or detergent. Whereas the interaction between Nup98 and Nup93 was sensitive to either Tween or TX-100, binding persisted in the presence of HD. We conclude that binding to Nup93 accounts for the HD-resistant NPC targeting activity of the GLFG domain and is distinct from GLFG function in the permeability barrier, a property of the NPC that is disrupted by HD treatment.

DISCUSSION

We used FRAP to conduct in vivo comparisons of nucleoporin FG repeat domain cohesion. We chose to focus on repeat domains from Nup214, Nup98, Nup62, and Nup153 as representatives of the cytoplasmic face/filaments, the central core, and the nuclear basket of the NPC. Our results indicate that the repeat domain of Nup98, the only one to contain GLFG repeats, is substantially more cohesive than repeat domains from the other nucleoporins tested. In addition, our results with Nup98 shed new light on the multiple interactions of this nucleoporin with the NPC.

On the basis of our data, we conclude that Nup98 participates in at least three distinct types of interaction at the NPC. First, the major NPC-targeting determinant lies in the structured region (amino acids 711–863) that interacts with Nup96, the second protein derived from
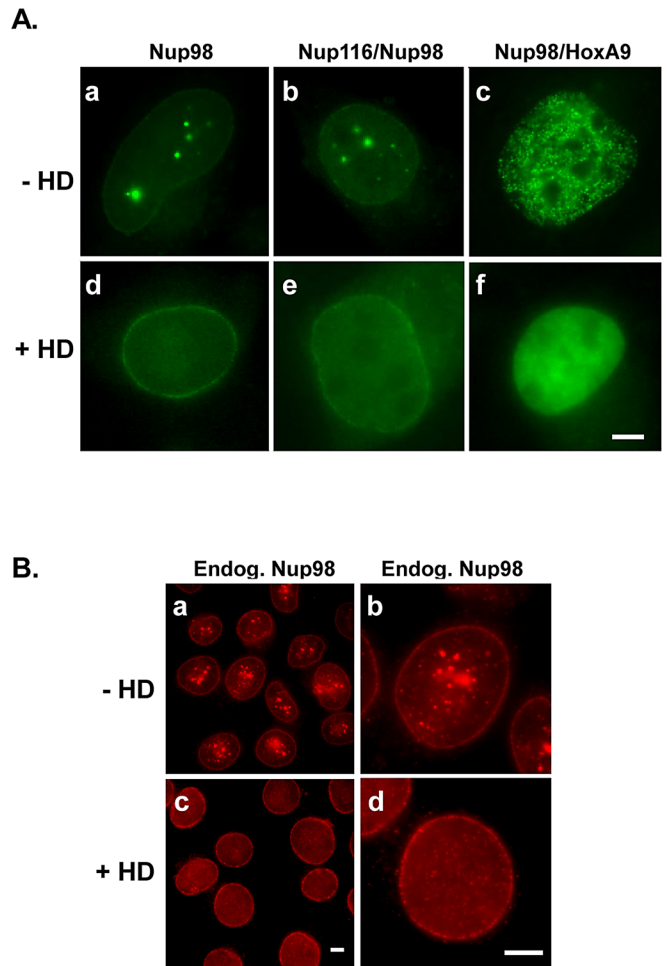
FIGURE 5: Interaction between GLFG repeats is sensitive to hexanediol. (A) Intranuclear GLFG bodies or Nup98/HoxA9 foci are dispersed by brief treatment of cells with HD. GFP-tagged proteins were transiently expressed and imaged by widefield microscopy before (a–c) or after (d–f) 30-s treatment with 5% HD. (B) Endogenous Nup98 GLFG bodies are dispersed by HD treatment. Nup98 in HeLa-C cells was detected by Nup98 antibody before (a, b) or after (c, d) HD treatment.

autoproteolytic cleavage of the Nup98/Nup96 precursor, and a member of the scaffolding Y-complex of the NPC (Fontoura *et al.*, 1999; Rosenblum and Blobel, 1999; Hodel *et al.*, 2002). This same site in Nup98 also interacts, in a mutually exclusive manner, with Nup88 (Griffis *et al.*, 2003; Yoshida *et al.*, 2011). The Nup98 GLFG domain participates in two additional types of interactions: 1) cohesive interactions between repeat domains, which we modeled using intranuclear foci, and 2) binding to the nonrepeat nucleoporin, Nup93. The cohesive interaction between Nup98 repeats, like the functional permeability barrier of the NPC, is sensitive to treatment with HD. In contrast, binding between Nup98 and Nup93, like the localization of Nup98 to the NPC, is resistant to HD. Therefore it is most likely that binding of the Nup98 repeats to Nup93 accounts for much of the contribution of the repeat domain to NPC targeting. When fused to the Nup98 C-terminus, repeat domains from other nucleoporins were not able to enhance association with the NPC above the level of the C-terminus alone. This agrees with prior reports that ScNic96, the Nup93 orthologue in *S. cerevisiae*, binds specifically to GLFG repeat domains (Patel *et al.*, 2007; Schrader *et al.*, 2008). Whereas GLFG repeats are essential for interaction with Nup93 and enhancement of
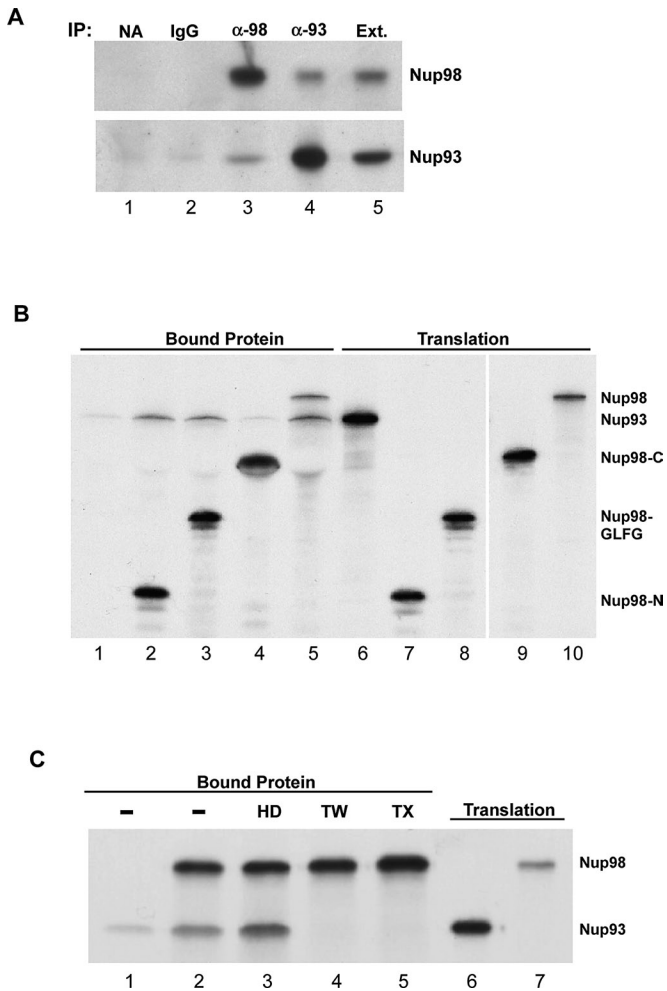
FIGURE 6: The Nup98 repeat domain interacts with Nup93 in a non–hexanediol-sensitive manner. (A) Nup98 and Nup93 can be coimmunoprecipitated. Nup98 or Nup93 was immunoprecipitated from *Xenopus* egg extract in the absence of detergent, and equal amounts of immunoprecipitate were analyzed by immunoblotting with antibodies to Nup98 or Nup93. (B) Nup93 binds to the repeat domains of Nup98. In vitro–translated Nup93 was incubated with unprogrammed translation reaction (lane 1), myc-tagged Nup98 fragments (Nup98-N, amino acids [aa] 1–225, lane 2; Nup98-GLFG, aa 220–506, lane 3; Nup98-C, aa 506–920, lane 4) or myc-tagged Nup98 (lane 5), and complexes were isolated on myc antibody beads and assessed by PAGE and autoradiography. Binding assays were carried out in the absence of detergent, leading to slight Nup93 background; however, Nup93 was significantly enriched on Nup98 or Nup98 fragments containing nucleoporin repeats (lanes 2, 3, and 5). (C) Binding of Nup93 to Nup98 is resistant to HD but sensitive to detergents. Binding assays were carried out as in B, using Nup93 alone (lane 1) or Nup93 together with myc-Nup98 (lanes 2–5). Bound proteins were isolated using myc antibody beads and washed well with buffer (lanes 1 and 2) or with buffer followed by one wash with 5% HD, 0.2% Tween-20 (TW, lane 4), or 0.2% TX-100 (TX, lane 5). Bound proteins were analyzed by PAGE and autoradiography.

NPC localization, we found that the total number of FG repeats also affects the apparent stability of the localization.

In the assembled NPC, the Y-complex, also referred to as "coat" nucleoporins, forms the outermost, juxtamembrane layer of the central core (Alber *et al.*, 2007; Hoelz *et al.*, 2011). The next-more-internal layer comprises "adapter" nucleoporins and includes

Nup93 and its subcomplex partners, Nup188 and Nup205, along with Nup155 and Nup35 (Grandi *et al.*, 1997; Miller *et al.*, 2000; Theerthagiri *et al.*, 2010). Through binding to components of each of these concentric layers, Nup98 is positioned with the C-terminus toward the outermost layer of the NPC core and the repeat domain toward the center. These interactions support our recent electron microscopy and structured illumination microscopy imaging, which puts both N- and C-termini of Nup98 near the center of the nucleo-cytoplasmic axis of the pore (Chatel *et al.*, 2012).

One goal of this study was to compare the relative cohesiveness of different vertebrate nucleoporin repeat domains in a cellular context. Previously, cohesive properties of nucleoporin repeats were assessed in vitro with a fluorescent bead halo assay (Patel and Rexach, 2008). This assay is extremely useful for testing low-affinity interactions, but a drawback is that nucleoporin fragments must be bacterially expressed and purified, potentially limiting the assay to soluble repeat domains or fragments.

We circumvented the need to express the relatively insoluble vertebrate nucleoporin repeat domains by measuring cohesion in vivo with a photobleaching assay. By expressing each domain as a GFP-tagged fusion with the homeodomain of HoxA9, we were able to analyze all domains in an identical context and also isolate the potential interactions in the nucleoplasm rather than at the NPC. Foci formed by wild-type Nup98 or Nup98/HoxA9 are readily distinguished by their intranuclear distribution patterns; however, with a difference of only one FG repeat (38 vs. 39), these have very similar dynamics by FRAP, suggesting that the nature of their interaction within foci is the same.

With these assays, we found that repeat domains from Nup153 and Nup62 do not form dynamic intranuclear bodies. The Nup62/HoxA9 fusion was always distributed diffusely throughout the nucleoplasm, and its recovery dynamics were almost identical to that of HoxA9 alone. This was somewhat surprising, given this nucleoporin's central location in the NPC (Schwarz-Herion *et al.*, 2007), major contribution to nuclear transport (Finlay *et al.*, 1991; Hulsmann *et al.*, 2012), and timing of assembly (Dultz *et al.*, 2008), which together suggested that Nup62 repeats might participate in a hydrophobic phase proposed to occupy the center of the NPC. It is formally possible that a higher local concentration of Nup62 achieved within the NPC facilitates such interaction. The Nup62 orthologue ScNsp1, which contains more than five times the number of repeats present in Nup62, was not cohesive in the bead halo assay (Patel *et al.*, 2007). However, unlike Nup62, the ScNsp1 FG domain can be divided into two subdomains, one of which is cohesive, the other noncohesive. Given the central location of both Nup98 and Nup62 within the NPC, we considered the possibility that repeat domains from the two proteins might interact with each other in a heterotypic manner. However, GFP-Nup62/HoxA9 was never recruited to endogenous GLFG bodies, nor did its overexpression disrupt GLFG body assembly (Desai and Powers, unpublished data). Thus it is unlikely the repeat domains of these two nucleoporins interact significantly with each other.

Nup153/HoxA9 was equilibrated between the nucleus and cytoplasm. When expressed independently, the Nup153 repeat domain was cytoplasmic, although nucleocytoplasmic shuttling was not tested (Bastos *et al.*, 1996). Our results suggest that the Nup153 repeat domain, possibly through its known interactions with a subset of transport factors (Shah and Forbes, 1998; Nakielny *et al.*, 1999), can counterbalance the NLS of the HoxA9 homeodomain (Xu and Powers, 2010). It has been proposed that the Nup153 repeat domain extends from its anchor point on the nuclear face through the central channel during transport (Fahrenkrog *et al.*, 2002; Paulillo

et al., 2005). In this role, a high degree of cohesiveness might be undesirable, as it could potentially trap the repeat domain within the channel and disrupt transport.

The Nup214 repeat domain was the only non-GLFG domain to form intranuclear bodies. Unlike the Nup98/HoxA9 fusion proteins, which were always found in nuclear foci, the formation of bodies by Nup214/HoxA9 was correlated with the level of expression. At the lowest levels, the Nup214 fusion was diffusely distributed throughout the nucleoplasm but coalesced into bodies as the expression level increased somewhat (Desai and Powers, unpublished data). In keeping with this, Nup214 fusions were less cohesive than Nup98 fusions, as measured by FRAP. Intriguingly, in 13 of the 36 FG motifs within the Nup214 fragment, valine (V) or L immediately precedes the FG (see Supplemental Tables S1 and S2 for summaries of human and yeast FG domain properties and Table S3 for a list of all human FG motifs). The majority of these hydrophobic-FG ((H)-FG) motifs are clustered in one region, in which 10 of 18 motifs are of this type and intervening spacer sequences entirely lack charged residues. Outside of the Nup98 GLFG domain, this density of (H)-FG motifs is seen only in Nup214 and in the transmembrane Nup, POM121 (Supplemental Table S3). We propose that these more hydrophobic motifs give the domain a region of lower but demonstrable cohesiveness.

The significance of a hydrophobic residue at this position is supported by the loss of cohesion when all L within a GLFG repeat domain fragment are mutated to A (Patel et al., 2007). Subsequently, the same GLFG repeats were mutated to FSFG with no loss of cohesion. The investigators concluded that a major determinant of cohesive nature is the uncharged nature of the spacers rather than the specific repeat motif. (Yamada et al., 2010). Taking this mutational analysis together with our measurements of human repeat domain cohesion, we propose two requirements for cohesive nucleoporin domains: 1) low charge density in spacers, and 2) a significant number of motifs with a hydrophobic residue (L, V, I, F, or, in rare cases, M) at position −1 or −2 relative to the FG. Thus FG motifs alone would be insufficient for cohesion, even within in an uncharged domain, whereas the number of (H)-FG repeats within a low-charge domain correlates well with the relative FRAP recovery rates we measured.

Possibly the motifs in huNup214 evolved to create a nucleoporin with intermediate cohesive properties. In contrast to huNup214, the yeast orthologue ScNup159 is not cohesive (Patel et al., 2007); only 4 of the 25 FG motifs are preceded by a hydrophobic residue, as described earlier, and lysines are found throughout the spacer sequences. Of interest, the domain organization also differs between these orthologues; although both contain an N-terminal β-propeller structure (Weirich et al., 2004; Napetschnig et al., 2007), the repeat domain is central in Nup159 but C-terminal in Nup214. The differences in both the positioning and properties of the repeat domains suggest that the mechanistic contribution of Nup214 to NPC function could differ somewhat from that of Nup159.

Overall our results indicate that Nup98 is ideally positioned and has properties consistent with a role in the NPC permeability barrier. A recent report described a significant functional contribution of Nup98 to permeability in reconstituted nuclei (Hulsmann et al., 2012). During the partly open mitosis of Aspergillus nidulans, a subset of nucleoporins, including Nup98, is released from the NPC scaffold, rendering the NPC permeable and facilitating equilibration between the mitotic cytosol and nucleoplasm (De Souza et al., 2004; Osmani et al., 2006). In cycling mammalian cells, Nup98 is the first nucleoporin to be released from the prophase NPC, just before permeability of the nuclear envelope is greatly increased (Dultz et al.,

2008). Although Nup98 association occurs about midway during NPC reassembly after mitosis, Nup93, Nup98, and Nup62 are incorporated in rapid succession, and their association correlates with the initiation of nuclear import.

Like the NPC and the permeability barrier, GLFG bodies also disassemble at mitosis; this raises the possibility of a common signal that triggers dissociation of repeats, both within the nucleoplasm and at the NPC. Nup98 is a target of multiple phosphorylations at mitosis; however, these were confined to the C-terminal domain and not found within the repeats (Laurell et al., 2011). A second posttranslational modification of Nup98, O-linked GlcNAc, occurs within repeat domains, but we have not been able to establish a change in this modification at mitosis. Perhaps other modifications remain to be mapped within the repeat domain that will influence the cohesiveness of repeats.

In summary, we showed that the GLFG repeat domain of human Nup98 is the most cohesive of those tested, although a region of the Nup214 domain has lesser but detectable interactions. Given its localization, timing of assembly and disassembly from the NPC, and sensitivity of cohesion between repeats to HD, Nup98 likely contributes substantially to both the permeability barrier of the NPC and cargo translocation.

MATERIALS AND METHODS
DNA constructs
GFP-Nup98 (amino acids 1–920), GFP-Nup98 N-term (1–225), GFP-Nup98GLFG (221–504), GFP-Nup98 C-term (506–920), GFP-Nup98/HoxA9, cyan fluorescent protein (CFP)–Nup98/PMX1, GFP-HoxA9, and GFP-HoxA9 C-term were described previously (Griffis et al., 2002; Xu and Powers, 2010). Other domain constructs—GFP-Nup98-N (1–225), GFP-Nup98-GLFG(C) (369–469), GFP-Nup98-GLFG (222–469), GFP-Nup98-GBD-GLFG (156–469), and GFP-Nup98-N-GLFG(C)—were produced by excision and religation from GFP-Nup98/HoxA9 using existing sites. Equivalent constructs carrying the Nup98 C-terminal domain were produced in the same manner by excision from GFP-Nup98.

To generate GFP-Nup98-2xGLFG/HoxA9, a fragment of Nup98 (225–505) was amplified by PCR and substituted for the Nup98 fragment (1–221) in GFP-Nup98/HoxA9. Repeat domains of Nup62 (1–306), Nup153 (900–1419), Nup214 (1632–2090), and Nup116 (181–725) were produced by PCR and substituted for Nup98 in either GFP-Nup98 or GFP-Nup98/HoxA9 to create C-terminal or HoxA9 fusions, respectively. To create GFP-Nup153(H)/Nup98 and GFP-Nup214(H)/Nup98, fragments of Nup153 (900–1215) and Nup214 (1876–2090) were excised from GFP-Nup153/Nup98 and GFP-Nup214/Nup98, respectively.

All subcloning was performed by standard protocols (Sambrook et al., 1989). Site-mutagenesis was carried out by QuikChange mutagenesis (Stratagene, La Jolla, CA). Constructs were confirmed by DNA sequencing.

Cell culture and immunofluorescence
HeLa cells and HeLa-C cells (a kind gift of Volker Cordes, Max Planck Institute, Goettingen, Germany) were cultured in high-glucose DMEM with 10% fetal bovine serum supplemented with glutamine and antibiotics. Either FuGENE (Roche Diagnostics, Indianapolis, IN) or Lipofectamine 2000 (Invitrogen, Carlsbad, CA) was used for transient transfection according to the manufacturer's instruction. From 0.2 to 0.5 μg of DNA per well in six-well plates was used for transfections. Immunofluorescence staining was carried out as described previously (Xu and Powers, 2010). Anti–Nup98 C-terminus (1:2000; Griffis et al., 2002) was used to detect endogenous Nup98;

this does not recognize Nup98/HoxA9 fusions. For hexanediol treatments, cells on coverslips were incubated with 5% 1,6-hexanediol (Acros Organics/Fisher Scientific, Pittsburgh, PA) in water for 30 s, rinsed in phosphate-buffered saline (PBS), and immediately fixed for immunostaining.

Images were captured by either a BX60 microscope (Olympus, Tokyo, Japan) equipped with a 12-bit camera (Hamamatsu Photonics, Hamamatsu City, Japan) and SlideBook software (Intelligent Imaging Innovations, Denver, CO) or a Zeiss LSM510 confocal microscope (Carl Zeiss, Thornwood, NY). For simultaneous detection of GFP and CFP, a Zeiss LSM510 Meta-equipped confocal microscope was used as described previously (Xu and Powers, 2010).

Fluorescence recovery after photobleaching

FRAP analysis was carried out on a Zeiss LSM510 confocal microscope as described previously (Xu and Powers, 2010). Briefly, HeLa cells were plated and transfected in LabTek II chambered coverslips (Nalgene, Rochester, NY). Imaging medium (DMEM with 20% fetal calf serum and 25 mM 4-(2-hydroxyethyl)-1-piperazineethanesulfonic acid [HEPES], pH 7.0) was substituted for the normal medium before imaging. Cells chosen for FRAP analysis had low to moderate GFP-protein levels. At high expression levels, aggregates were sometimes seen in the cytoplasm, but these were generally not dynamic, suggesting that they are artifacts of overexpression, and they were not used in analysis. FRAP recovery data were analyzed using Origin 6.1 software (OriginLab, Northampton, MA).

Coimmunoprecipitations and in vitro binding assays

For immunoprecipitations, 30 μl of TrueBlot anti-rabbit beads (eBioscience, San Diego, CA) was incubated with Block solution (10 mg/ml bovine serum albumin [BSA], 5 mg/ml casamino acids in 1× PBS) for 1 h at 4° C. Either anti–*Xenopus* Nup98 or anti–*Xenopus* Nup93, 15 μg, was diluted in 1 ml of Block solution with 1 mM dithiothreitol (DTT) and 1× Complete Protease Inhibitor (Roche, Nutley, NJ) and incubated overnight 4°C with preblocked beads. After three washes with ELBs buffer (10 mM HEPES, 2.5 mM MgCl$_2$, 50 mM KCl, pH 7.4), beads were incubated with 500 μl of diluted *Xenopus* egg extract (1:50 dilution in ELBs containing DTT and 1× Complete Protease Inhibitor) for 2 h at 4°C. Samples were washed five times in ELBs and three times in 25 mM Tris-HCl (pH 7.4) before being eluted from beads with SDS gel sample buffer. Diluted *Xenopus* egg extract was precleared by incubation for 1 h at 4°C with 30 μl of blocked TrueBlot anti-rabbit beads before use. The following antibodies were used for Western blots: anti-GLFG (1:6000; Sigma-Aldrich, St. Louis, MO), anti–*Xenopus* Nup93 (1:1500), anti-rabbit TrueBlot horseradish peroxidase (HRP) (1:1000; eBioscience), and anti-mouse TrueBlot HRP (1:1000; eBioscience).

For in vitro binding assays, expression constructs were translated using the TNT-coupled reticulocyte lysate system (Promega; Madison, WI) supplemented with [^{35}S]methionine (PerkinElmer, Waltham, MA). A 10-μl amount of translated Nup98 or Nup98 fragments was incubated with 10 μl of translated Nup93 for 1 h at room temperature and then diluted in 300 μl of PBS with 10 mg/ml BSA and 1× Complete Protease Inhibitor (Roche). A 1-μg amount of anti-myc (Developmental Studies Hybridoma Bank, Iowa City, IA) and 25 μl of preblocked protein A–Sepharose beads (Sigma-Aldrich) were added and incubated for 2 h at 4°C. Beads were washed five times with 2 mg/ml BSA in PBS and eluted from beads with SDS gel sample buffer. When included, 0.2% Triton X-100, 0.2% Tween-20, or 5% hexanediol was used for the final wash of beads before elution.

REFERENCES
Alber F *et al.* (2007). The molecular architecture of the nuclear pore complex. Nature 450, 695–701.

Bastos R, Lin A, Enarson M, Burke B (1996). Targeting and function in mRNA export of nuclear pore complex protein Nup153. J Cell Biol 134, 1141–1156.

Bayliss R, Littlewood T, Stewart M (2000). Structural basis for the interaction between FxFG nucleoporin repeats and importin-beta in nuclear trafficking. Cell 102, 99–108.

Chatel G, Desai SH, Mattheyses AL, Powers MA, Fahrenkrog B (2012). Domain topology of nucleoporin Nup98 within the nuclear pore complex. J Struct Biol 177, 81–89.

Chook YM, Suel KE (2011). Nuclear import by karyopherin-betas: recognition and inhibition. Biochim Biophys Acta 1813, 1593–1606.

Chow KH, Elgort S, Dasso M, Ullman KS (2012). Two distinct sites in Nup153 mediate interaction with the SUMO proteases SENP1 and SENP2. Nucleus 3, 349–358.

De Souza CP, Osmani AH, Hashmi SB, Osmani SA (2004). Partial nuclear pore complex disassembly during closed mitosis in *Aspergillus nidulans*. Curr Biol 14, 1973–1984.

Denning DP, Patel SS, Uversky V, Fink AL, Rexach M (2003). Disorder in the nuclear pore complex: the FG repeat regions of nucleoporins are natively unfolded. Proc Natl Acad Sci USA 100, 2450–2455.

Dultz E, Zanin E, Wurzenberger C, Braun M, Rabut G, Sironi L, Ellenberg J (2008). Systematic kinetic analysis of mitotic dis- and reassembly of the nuclear pore in living cells. J Cell Biol 180, 857–865.

Dundr M, Misteli T (2003). Measuring dynamics of nuclear proteins by photobleaching. Curr Protoc Cell Biol Chapter 13, Unit 13.5.

Fahrenkrog B, Maco B, Fager AM, Koser J, Sauder U, Ullman KS, Aebi U (2002). Domain-specific antibodies reveal multiple-site topology of Nup153 within the nuclear pore complex. J Struct Biol 140, 254–267.

Finlay DR, Meier E, Bradley P, Horecka J, Forbes DJ (1991). A complex of nuclear pore proteins required for pore function. J Cell Biol 114, 169–183.

Fontoura BM, Blobel G, Matunis MJ (1999). A conserved biogenesis pathway for nucleoporins: proteolytic processing of a 186-kilodalton precursor generates Nup98 and the novel nucleoporin, Nup96. J Cell Biol 144, 1097–1112.

Frey S, Richter RP, Gorlich D (2006). FG-rich repeats of nuclear pore proteins form a three-dimensional meshwork with hydrogel-like properties. Science 314, 815–817.

Grandi P, Dang T, Pane N, Shevchenko A, Mann M, Forbes D, Hurt E (1997). Nup93, a vertebrate homologue of yeast Nic96p, forms a complex with a novel 205-kDa protein and is required for correct nuclear pore assembly. Mol Biol Cell 8, 2017–2038.

Griffis ER, Altan N, Lippincott-Schwartz J, Powers MA (2002). Nup98 is a mobile nucleoporin with transcription-dependent dynamics. Mol Biol Cell 13, 1282–1297.

Griffis ER, Xu S, Powers MA (2003). Nup98 localizes to both nuclear and cytoplasmic sides of the nuclear pore and binds to two distinct nucleoporin subcomplexes. Mol Biol Cell 14, 600–610.

Guan T, Müller S, Klier G, Panté N, Blevitt JM, Haner M, Paschal B, Aebi U, Gerace L (1995). Structural analysis of the p62 complex, an assembly of O-linked glycoproteins that localizes near the central gated channel of the nuclear pore complex. Mol Biol Cell 6, 1591–1603.

Hodel A, Hodel M, Griffis E, Hennig K, Ratner G, Xu S, Powers M (2002). The three-dimensional structure of the autoproteolytic, nuclear pore-targeting domain of the human nucleoporin nup98. Mol Cell 10, 347–358.

Hoelz A, Debler EW, Blobel G (2011). The structure of the nuclear pore complex. Annu Rev Biochem 80, 613–643.

Hu T, Guan T, Gerace L (1996). Molecular and functional characterization of the p62 complex, an assembly of nuclear pore complex glycoproteins. J Cell Biol 134, 589–601.

Hulsmann BB, Labokha AA, Gorlich D (2012). The permeability of reconstituted nuclear pores provides direct evidence for the selective phase model. Cell 150, 738–751.

Hutten S, Kehlenbach RH (2007). CRM1-mediated nuclear export: to the pore and beyond. Trends Cell Biol 17, 193–201.

Laurell E, Beck K, Krupina K, Theerthagiri G, Bodenmiller B, Horvath P, Aebersold R, Antonin W, Kutay U (2011). Phosphorylation of Nup98 by multiple kinases is crucial for NPC disassembly during mitotic entry. Cell 144, 539–550.

Lim RY, Fahrenkrog B, Koser J, Schwarz-Herion K, Deng J, Aebi U (2007). Nanomechanical basis of selective gating by the nuclear pore complex. Science 318, 640–643.

Lippincott-Schwartz J, Snapp E, Kenworthy A (2001). Studying protein dynamics in living cells. Nat Rev Mol Cell Biol 2, 444–456.

Mackay DR, Makise M, Ullman KS (2010). Defects in nuclear pore assembly lead to activation of an Aurora B-mediated abscission checkpoint. J Cell Biol 191, 923–931.

Marfori M, Mynott A, Ellis JJ, Mehdi AM, Saunders NF, Curmi PM, Forwood JK, Boden M, Kobe B (2011). Molecular basis for specificity of nuclear import and prediction of nuclear localization. Biochim Biophys Acta 1813, 1562–1577.

Miller BR, Powers M, Park M, Fischer W, Forbes DJ (2000). Identification of a new vertebrate nucleoporin, nup188, with the use of a novel organelle trap assay. Mol Biol Cell 11, 3381–3396.

Nakielny S, Shaikh S, Burke B, Dreyfuss G (1999). Nup153 is an M9-containing mobile nucleoporin with a novel Ran-binding domain. EMBO J 18, 1982–1995.

Napetschnig J, Blobel G, Hoelz A (2007). Crystal structure of the N-terminal domain of the human protooncogene Nup214/CAN. Proc Natl Acad Sci USA 104, 1783–1788.

Onischenko E, Weis K (2011). Nuclear pore complex-a coat specifically tailored for the nuclear envelope. Curr Opin Cell Biol 23, 293–301.

Osmani AH, Davies J, Liu HL, Nile A, Osmani SA (2006). Systematic deletion and mitotic localization of the nuclear pore complex proteins of *Aspergillus nidulans*. Mol Biol Cell 17, 4946–4961.

Patel SS, Rexach MF (2008). Discovering novel interactions at the nuclear pore complex using bead halo: a rapid method for detecting molecular interactions of high and low affinity at equilibrium. Mol Cell Proteomics 7, 121–131.

Patel SS, Belmont BJ, Sante JM, Rexach MF (2007). Natively unfolded nucleoporins gate protein diffusion across the nuclear pore complex. Cell 129, 83–96.

Paulillo SM, Phillips EM, Koser J, Sauder U, Ullman KS, Powers MA, Fahrenkrog B (2005). Nucleoporin domain topology is linked to the transport status of the nuclear pore complex. J Mol Biol 351, 784–798.

Peters R (2005). Translocation through the nuclear pore complex: selectivity and speed by reduction-of-dimensionality. Traffic 6, 421–427.

Pritchard CE, Fornerod M, Kasper LH, van Deursen JM (1999). RAE1 is a shuttling mRNA export factor that binds to a GLEBS-like NUP98 motif at the nuclear pore complex through multiple domains. J Cell Biol 145, 237–254.

Ribbeck K, Gorlich D (2001). Kinetic analysis of translocation through nuclear pore complexes. EMBO J 20, 1320–1330.

Ribbeck K, Gorlich D (2002). The permeability barrier of nuclear pore complexes appears to operate via hydrophobic exclusion. EMBO J 21, 2664–2671.

Rosenblum JS, Blobel G (1999). Autoproteolysis in nucleoporin biogenesis. Proc Natl Acad Sci USA 96, 11370–11375.

Rout MP, Aitchison JD, Magnasco MO, Chait BT (2003). Virtual gating and nuclear transport: the hole picture. Trends Cell Biol 13, 622–628.

Rout MP, Aitchison JD, Suprapto A, Hjertaas K, Zhao Y, Chait BT (2000). The yeast nuclear pore complex: composition, architecture, and transport mechanism. J Cell Biol 148, 635–651.

Sambrook J, Fritsch EF, Maniatis T (1989). Molecular Cloning: A Laboratory Manual, Cold Spring Harbor, NY: Cold Spring Harbor Laboratory Press.

Schrader N, Stelter P, Flemming D, Kunze R, Hurt E, Vetter IR (2008). Structural basis of the nic96 subcomplex organization in the nuclear pore channel. Mol Cell 29, 46–55.

Schwarz-Herion K, Maco B, Sauder U, Fahrenkrog B (2007). Domain topology of the p62 complex within the 3-D architecture of the nuclear pore complex. J Mol Biol 370, 796–806.

Shah S, Forbes DJ (1998). Separate nuclear import pathways converge on the nucleoporin nup153 and can be dissected with dominant-negative inhibitors. Curr Biol 8, 1376–1386.

Shulga N, Goldfarb DS (2003). Binding dynamics of structural nucleoporins govern nuclear pore complex permeability and may mediate channel gating. Mol Cell Biol 23, 534–542.

Strawn LA, Shen T, Shulga N, Goldfarb DS, Wente SR (2004). Minimal nuclear pore complexes define FG repeat domains essential for transport. Nat Cell Biol 6, 197–206.

Terry LJ, Wente SR (2009). Flexible gates: dynamic topologies and functions for FG nucleoporins in nucleocytoplasmic transport. Eukaryot Cell 8, 1814–1827.

Theerthagiri G, Eisenhardt N, Schwarz H, Antonin W (2010). The nucleoporin Nup188 controls passage of membrane proteins across the nuclear pore complex. J Cell Biol 189, 1129–1142.

Walde S, Kehlenbach RH (2010). The part and the whole: functions of nucleoporins in nucleocytoplasmic transport. Trends Cell Biol 20, 461–469.

Weirich CS, Erzberger JP, Berger JM, Weis K (2004). The N-terminal domain of Nup159 forms a beta-propeller that functions in mRNA export by tethering the helicase Dbp5 to the nuclear pore. Mol Cell 16, 749–760.

Xu S, Powers MA (2010). Nup98-homeodomain fusions interact with endogenous Nup98 during interphase and localize to kinetochores and chromosome arms during mitosis. Mol Biol Cell 21, 1585–1596.

Yamada J et al. (2010). A bimodal distribution of two distinct categories of intrinsically disordered structures with separate functions in FG nucleoporins. Mol Cell Proteomics 9, 2205–2224.

Yang W (2011). "Natively unfolded" nucleoporins in nucleocytoplasmic transport: clustered or evenly distributed? Nucleus 2, 10–16.

Yoshida K, Seo HS, Debler EW, Blobel G, Hoelz A (2011). Structural and functional analysis of an essential nucleoporin heterotrimer on the cytoplasmic face of the nuclear pore complex. Proc Natl Acad Sci USA 108, 16571–16576.